AD-A053 553 COLORADO STATE UNIV FORT COLLINS DEPT OF CHEMISTRY F/G 7/4
ABSORPTION AND ELECTRONIC RAMAN SCATTERING SPECTRA OF THE GAMMA--ETC(U)
MAR 78 E R BERNSTEIN, J D WEBB N00014-75-C-1179
UNCLASSIFIED TR-17 NL

1 OF 1
AD A053 553

END
DATE FILMED
6-78
DDC

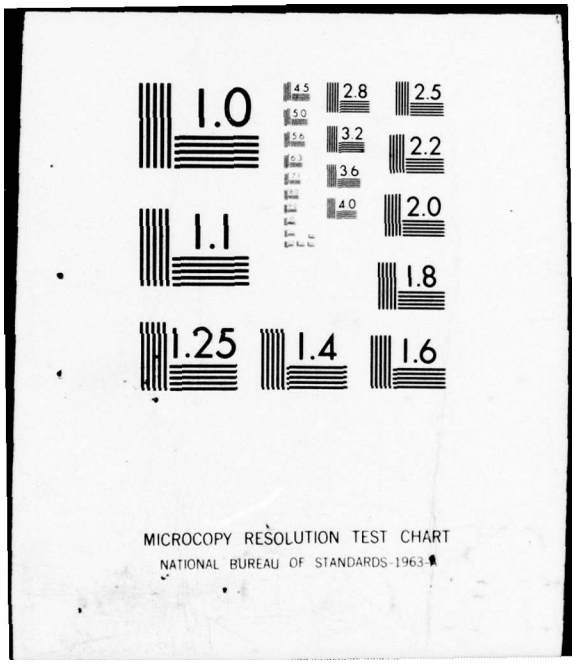
1.0
1.1
1.25
1.4
1.6
1.8
2.0
2.2
2.5
2.8
3.2
3.6
4.0
4.5
5.0
5.6
MICROCOPY RESOLUTION TEST CHART
NATIONAL BUREAU OF STANDARDS-1963-A

OFFICE OF NAVAL RESEARCH

Contract N00014-75-C-1179

Task No. NR 056-607

TECHNICAL REPORT NO. 17

"ABSORPTION AND ELECTRONIC RAMAN SCATTERING SPECTRA OF THE Γ_{8g} ($^2T_{1g}$) STATE OF IrF_6 AT 1.6μ - A RESOLUTION OF THE JAHN-TELLER PROBLEM"

by

E. R. Bernstein and J. D. Webb

Prepared for Publication
in
Molecular Physics

Department of Chemistry
Colorado State University
Fort Collins, Colorado 80523

March 1978

UNCLASSIFIED

SECURITY CLASSIFICATION OF THIS PAGE (When Data Entered)

REPORT DOCUMENTATION PAGE	READ INSTRUCTIONS BEFORE COMPLETING FORM
1. REPORT NUMBER (14) TR-17 ✓	2. GOVT ACCESSION NO. / 3. RECIPIENT'S CATALOG NUMBER
4. TITLE (and Subtitle) (6) Absorption and Electronic Raman Scattering Spectra of the Γ_{8g} State of IrF_6^- at 1.6μ - A Resolution of the Jahn-Teller Problem. micrometers	5. TYPE OF REPORT & PERIOD COVERED (9) Technical Report,
	6. PERFORMING ORG. REPORT NUMBER
7. AUTHOR(s) (10) E. R./Bernstein [redacted] J. D./Webb Gamma sub 8g (15)	8. CONTRACT OR GRANT NUMBER(s) N00014-75-C-1179 ✓
9. PERFORMING ORGANIZATION NAME AND ADDRESS Department of Chemistry Colorado State University Fort Collins, Colorado 80523 ✓	10. PROGRAM ELEMENT, PROJECT, TASK AREA & WORK UNIT NUMBERS NR 056-607
11. CONTROLLING OFFICE NAME AND ADDRESS Office of Naval Research Arlington, VA 22217	12. REPORT DATE (11) Mar[redacted]978 ✓
	13. NUMBER OF PAGES 36 (12) 35p.
14. MONITORING AGENCY NAME & ADDRESS (if different from Controlling Office)	15. SECURITY CLASS. (of this report) Unclassified
	15a. DECLASSIFICATION/DOWNGRADING SCHEDULE

16. DISTRIBUTION STATEMENT (of this Report)

Approved for Public Release; Distribution Unlimited.

17. DISTRIBUTION STATEMENT (of the abstract entered in Block 20, if different from Report)

18. SUPPLEMENTARY NOTES

19. KEY WORDS (Continue on reverse side if necessary and identify by block number)

IrF_6
$\Gamma_8 (t_{2g})^3$ states
Jahn-Teller Effect
Electronic Raman scattering
Absorption spectra
Gamma sub 8g
sub 1g

20. ABSTRACT (Continue on reverse side if necessary and identify by block number)

Electronic Raman scattering and absorption spectra are presented which allow an interpretation of the vibronic structure of the Γ_{8g} ($^2T_{1g}$) excited electronic state of IrF_6^- at 1.6μ. micrometers Large splittings and shifts are observed for the Jahn-Teller active ν_2 (e_g), ν_5 (t_{2g}), and $2\nu_5$ vibrations. From → next pg
sub g sub 2g

DD FORM 1 JAN 73 1473 EDITION OF 1 NOV 65 IS OBSOLETE S/N 0102-014-6601

nu 5

UNCLASSIFIED

SECURITY CLASSIFICATION OF THIS PAGE (When Data Entered)

nu 2

404 992

20. (continued...)

these spectra linear (D_2^{Γ} and D_5^{Γ}) and quadratic ($Q_2^{\Gamma}[a_{1g}]$, $Q_2^{\Gamma}[e_g]$, $Q_5^{\Gamma}[a_{1g}]$, $Q_5^{\Gamma}[e_g]$, $Q_5^{\Gamma}[t_{2g}]$) Jahn-Teller parameters can be determined. These data are compared with previously obtained parameters for the ReF_6^{Γ} ground state and the IrF_6^{Γ} ($^2T_{2g}$) at 0.6μ.

I. INTRODUCTION

This paper is one of a series in which the Jahn-Teller (JT) effect in metal hexafluorides is investigated.[1-3] The general conclusion drawn in the earlier work is that the usual linear JT theory is not an adequate one for these systems. Quadratic or higher order terms in the vibronic Hamiltonian are required. The present study of the Γ_{8g} ($^2T_{1g}$) electronic state of IrF_6 (~16,400 Å) offers an opportunity to test the generality of that conclusion and further helps to define the types of JT behavior possible for metal hexafluorides. It will be of interest, therefore, to compare and contrast the JT behavior of the Γ_{8g} ($^2T_{1g}$) state with that of the Γ_{8g} ground state of ReF_6[1] and the Γ_{8g} ($^2T_{2g}$) (~6800 Å) state of IrF_6.[2]

Previous work on the Γ_{8g} ($^2T_{1g}$) state of neat IrF_6 has been carried out;[4] however, as discussed earlier[2], neat crystal spectra suffer from many difficulties. In the present work, better data are obtained by employing mixed crsytals (IrF_6/MoF_6). Another important experimental advantage in this present work is that both absorption and electronic Raman spectroscopy have been utilized. The concomitant differences in selection rules between the two spectroscopic techniques provides an invaluable aid in assigning the complex Γ_{8g} ($^2T_{1g}$) spectrum. It might be noted that with the current availability of good photomultiplier tubes with excellent red-near IR response and high power gas and dye lasers, the usefulness of electronic Raman scattering for systems with electronic states in the IR-near IR and perhaps even the visible is much greater than its current utilization would indicate.

The theoretical and calculational methods necessary for understanding the Γ_{8g} ($^2T_{1g}$) spectrum are contained in the earlier papers.[1,2] The first

paper in this series on ReF_6[1] contains a review of basic JT theory as well as discussions of the effects of low symmetry electronic crystal fields on JT systems and the importance of simultaneous treatment of the ν_5 (t_{2g}) and ν_2 (e_g) JT-active vibrations. Matrix elements necessary for the ν_2-ν_5 linear JT calculation are given in reference 1. A qualitative symmetry-based theory (General Vibronic Coupling-GVC) applicable to those cases in which the linear JT theory fails is also discussed in this paper. Reference 2 treats the Γ_{8g} ($^2T_{2g}$) state of IrF_6 and contains detailed information concerning the electronic, vibrational, and crystal properties of IrF_6. Linear and quadratic JT parameters are also defined and discussed in these references; the linear parameters are D_5 and D_2 and the quadratic ones are Q_5 [a_{1g}], Q_5 [e_g], Q_5 [t_{2g}], Q_2 [a_{1g}] and Q_2 [e_g]. Subscripts 5 and 2 refer to the ν_5 and ν_2 modes, respectively.

II. EXPERIMENTAL

The two samples used in the experiment (0.5% and 5% IrF_6/MoF_6) were prepared by previously reported methods.[5] The absorption spectra were taken at superfluid helium temperatures (~1.6 K) with a 1 m monochromator, a liquid nitrogen-cooled InAs infrared detector and a tungsten-iodine lamp operated at constant current. The light from the lamp was dispersed by the monochromator before impinging on the sample in order to avoid sample heating. Under these conditions the sample remained at ca. 1.5 K and the 5 cm^{-1} hot band of IrF_6[2] did not congest the observed spectrum. The slitwidths used in the experiment varied from 0.6 cm^{-1} up to 1.6 cm^{-1} depending on line width and available intensity.

A continuous wave Ar^+ pumped dye laser employing disodium fluorescein as the active medium was used to excite the electronic Raman spectrum. The available Ar^+ laser lines cannot be readily employed for these experiments due to either absorption of the exciting light by the charge-transfer band (~5000 Å) or self-absorption of the Raman scattered light by the Γ_{7g} ($^2T_{2g}$) band (~8000 Å). These problems were avoided by using either 5400 Å or 5500 Å exciting laser radiation at powers of 500 mW - 1 W. A 0.5 m double monochromator with a cooled RCA C31034A photomultiplier tube, operated in the photon counting mode, was used to detect the Raman signal. Due to the weakness of the electronic Raman signal, slitwidths had to be quite large. Most spectra were taken with slitwidths corresponding to about 10 cm^{-1}. The upper wavelength limit of the photomultiplier tube (~8500 Å) proved to be the upper limit for the electronic Raman spectrum, but since the entire fundamental region [Γ_{8g} ($^2T_{1g}$) + (0-700 cm^{-1})] was accessible, this led to no essential difficulty. Background signals were found to originate from two sources:

Pyrex glass and ice. Thus, quartz sample cells and a metal dewar with quartz windows were used, and great care was taken to exclude ice.

III. RESULTS AND DISCUSSION

The electronic Raman and near infrared absorption data are presented in Tables 1 and 2. Some representative spectra are given in Figures 1-6.

It is helpful to discuss the selection rules and expected intensity ratios for electronic Raman scattering since the data are so important to the understanding of the complex Γ_{8g} ($^2T_{1g}$) spectra. Koningstein[6] has shown that for non-degenerate electronic states pure electronic Raman scattering intensity is much higher than the corresponding vibronic intensity. In the case of a degenerate electronic state, however, it has been shown that the Raman intensity from the pure electronic transition can be distributed over the vibronic portion of the spectrum by a JT effect.[7] It is expected, therefore, that the Raman spectrum of the Γ_{8g} ($^2T_{2g}$) manifold will exhibit a strong origin transition and observable ν_2 (e_g) and ν_5 (t_{2g}) peaks. The expectation is further strengthened by noting that if IrF_6 had perfect octahedral symmetry in the MoF_6 host crystal instead of only the C_s site symmetry, rigorous g-g Raman selection rule would only allow transitions to $\{\Gamma_{8g} + (\nu_1\ (a_{1g}), \nu_2\ (e_g)$, or $\nu_5\ (t_{2g}))\}$ vibronic states. Since the crystal site effects leading to the C_s symmetry are small, it is expected that the g-g selection rule will still be approximately correct.[8] It is not clear based on these considerations whether the totally symmetric mode ν_1 should be observed.

Using the above arguments and being aware that a JT interaction might occur in the degenerate electronic state, assignment of the electronic Raman spectrum is straightforward. The crystal-field split origin (Figure 1) is easily identified by its intensity and sharpness; it is further corroborated by comparison with the absorption data (Table 2). It should be noted that the observed splitting of the origin in Raman scattering is only 28 cm^{-1} whereas

in direct absorption, the splitting is measured as 34.6 cm^{-1}. The difference, ~6 cm^{-1}, is reminescent of the ground state splitting of 5.3 cm^{-1} and suggests the following explanation: the electronic Raman sample was probably not at the bath temperature (1.6 K) due to local heating by the laser beam. Sample heating explains the observations if it is assumed that the relevant hot band transition has a greater Raman intensity than the corresponding cold transition. Five of the six observed transitions in the vibrational bending region of the spectrum ($\Delta\sigma$(origin) ~200 - 300 cm^{-1}, see Figure 2) are assigned as vibronic components of ν_5 (t_{2g}); the other is ν_5 (a, host). Similarly, four of the five peaks in the stretching region (600-700 cm^{-1}) are identified as ν_2 components; the remaining peak is assigned as ν_3 (a, host) (see Table 1, Figure 3, and reference 5).

The absorption data (Table 2), due to different selection rules, contain transitions other than the JT-active vibrations; these will be examined first. The ν_6 (t_{2u}) bending vibration is easily located at 202.6 cm^{-1} since this frequency is not observed in the electronic Raman spectrum and its crystal field partner is found 34.8 cm^{-1} away at 237.4 cm^{-1} (origin splitting: 34.6 cm^{-1}). The equality of the two electronic crystal field splittings is indicative of a non-JT vibration.[1] Identification of ν_4 (t_{1u}) at 291.1 cm^{-1} is not as simple because its crystal field partner is not located at ca. 326 cm^{-1} (see Figure 4). The absence of the 326 cm^{-1} peak can, however, be rationalized if the effects of two-particle bands[2,5] are considered. It is suggested that the upper crystal field component of ν_4 has been subsumed in the ν_5 (a, host) two-particle band (318.4, 320.8, full width at half-height ~10 cm^{-1}). The intensity of this two-particle band lends credence to the conjecture, since the intensity of the transition at 312.5 cm^{-1} (a component of ν_5 which would be the most likely single particle state with which the two-particle state can mix) is not sufficient to account for the observed two-particle intensity.[5] The major

remaining non-JT-induced intensity is found at 700.4 cm^{-1} and is assigned as ν_1 (a_{1g}) rather than ν_3 (t_{1u}) because ν_6 (t_{2u}) and some ν_5 (t_{2g}) components are built on it.

Based on the above discussion, assignments of ν_2 (e_g) and ν_5 (t_{2g}) JT-split transitions can be made independently of the assignments made for the electronic Raman spectra. The vibrations ν_4 (t_{1u}), ν_5 (t_{2g}), and ν_6 (t_{2u}) are the bending vibrations (200-300 cm^{-1}); ν_4 and ν_6 have been assigned. Thus, the six remaining major features in the bending region may be taken as components of ν_5. The transitions in the bending mode combination region (400-600 cm^{-1}, Figure 5) are of particular interest since no signals above background were observed in the electronic Raman spectrum. Most of these are assigned as $2\nu_5$ components (see Table 2) because the various (ν_4, ν_5, ν_6) combinations and (ν_4, ν_6) overtones do not account for the observed number of peaks. (However, see discussion below as ν_2 ($J_2 = 3/2$) states overlap this region.)

Assignments in the stretching region (600-700 cm^{-1}) can also be made. The transitions at 685.8 and 692.0 cm^{-1} do not have normal crystal field partners (34.6 cm^{-1} to higher energy) and thus can be identified as ν_2 components. Two of the features at ca. 600 cm^{-1} are the $J_2 = 3/2$ components of ν_2 based on a comparison with the electronic Raman spectrum.

A comparison between the electronic Raman and absorption data is made in Table 3. Since most assignments were made independently, their overall agreement adds strength to the interpretation. The small differences observed can be explained as either due to uncertainties in the electronic Raman data caused by poor signal-to-noise ratio (e.g., ν_5^1 ($J_5 = 3/2$)) or differences in two-particle transition intensity patterns due to selection rules. As an example of the latter, compare the ~250 cm^{-1} ν_5 component in absorption (Figure 4) and electronic Raman scattering (Figure 2).

A theoretical understanding of the observed ν_2 and ν_5 JT-split vibrations is necessary in order to make more detailed assignments or extract parameter

values. It is probable that a coupled ν_2-ν_5 quadratic JT parametric calculation would meet these needs; however, the secular matrix for this difficult problem has not as yet been determined. Nonetheless, some of the above goals can be achieved by employing the presently available theoretical tools: ν_2-ν_5 linear JT secular matrix and GVC theory.[1] Examination of the data indicates that the ν_2 and ν_5 components appear in groups. The centers-of-gravity of these groups (Table 4) suggest the pattern expected for a linear JT effect. Thus, the data indicate that the linear coupling parameters, D_2 and D_5, are larger than the quadratic terms. The ν_2-ν_5 linear JT calculation can be employed to assign to the above groups of peaks the appropriate linear JT quantum numbers (J_2 or J_5) and also to obtain rough parameter values. The linear parameters D_2 and D_5 are determined explicitly in the coupled linear calculation. While they can generate the appropriate splitting between major line groupings (J_i = 3/2 and J_i = 1/2), an accurate center-of-gravity for the entire pattern is not obtained. An acceptable fit to the overall ν_2 and ν_5 patterns comes about with introduction of totally symmetric quadratic parameters Q_i [a_{1g}]. The effect of these particular quadratic terms in the Hamiltonian is to shift the center-of-gravity of the entire pattern by changing the apparent unperturbed vibrational frequency ν_i^0. The parameters which are varied are: (D_2, ν_2^0 (Q_2 [a_{1g}]), D_5, ν_5^0 (Q_5 [a_{1g}])) with ν_i^0 (Q_i [a_{1g}]) = $\nu_i^0\sqrt{(1 + Q_i\ [a_{1g}])}$.[1] The ν_i^0 are determined by comparison with other non-JT perturbed states. In this case, ν_5^0 ~275 cm^{-1} and ν_2^0 ~645 cm^{-1}. The results of the calculation are given in Table 4 and have been used in the assignments in Tables 1-3. The rough parameter values obtained are:

$$D_5 = 0.13$$

$$Q_5\ [a_{1g}] = -0.14,\ \nu_5^0\ (Q_5\ [a_{1g}]) = 255\ cm^{-1}$$

$$D_2 = 0.03$$

$$Q_2\ [a_{1g}] = -0.04,\ \nu_2^0\ (Q_2\ [a_{1g}]) = 630\ cm^{-1}$$

Within the framework of a coupled ν_2-ν_5 quadratic system, the [illegible] parameters account for all apparent shifts in centers-of-gravity of observed splitting patterns.

The GVC theory can be used to test the consistency of the interpretation since it predicts the number of components a given linear JT level generates under the action of higher order terms. It is also necessary to consider the effect of a low symmetry electronic crystal field on these levels. The Γ_{6g} and Γ_{7g} vibronic levels are Kramers doublets and are not split by electrostatic interactions, whereas Γ_{8g} level is split into two Kramers doublets by any low symmetry electrostatic field. A prediction of the number of components arising from each linear JT level can be made:

$$\nu_5\ (J_5 = 3/2) \rightarrow 4$$

$$\nu_5\ (J_5 = 1/2) \rightarrow 2$$

$$2\nu_5\ (J_5 = 5/2) \rightarrow 6$$

$$2\nu_5\ (J_5 = 1/2) \rightarrow 2$$

$$2\nu_5\ (J_5 = 3/2) \rightarrow 4$$

$$\nu_2\ (J_2 = 3/2) \rightarrow 2$$

$$\nu_2\ (J_2 = 1/2) \rightarrow 2.$$

These predictions are well borne out by the data except where Γ_{7g} Γ_{8g} and ν_2 $(J_2 = 3/2)$ overlap. Five of the expected six transitions are found, but since the peaks are broad ($\geq$ 10 cm^{-1}) it is possible that a near coincidence of peaks interferes with observation of the complete spectrum (see Figure 1).

It is interesting that all possible ν_2 and ν_5 components are observed, yet theory predicts that only Γ_{8g} vibronic states should have intensity in absorption. Apparently other intensity mechanisms, such as Fermi resonance or vibronic coupling which is allowed by the C_s site symmetry, are important. An additional example of one of these alternative intensity mechanisms being operative is

found in the near IR absorption spectrum of ReF_6 in which the $(\Gamma_{7g} + \nu_5) \leftarrow \Gamma_{8g}$ transition has much more intensity than expected.[1] It should be noted that previous work on the Γ_{8g} ($^2T_{1g}$) state of IrF_6[4] was hindered by lack of information in this regard; it had to be assumed that all ν_5 or ν_2 transitions were to a limited set of vibronic states ($J_2 = J_5 = 1/2$ in linear JT theory).

The other quadratic parameters (Q_5 [e_g], Q_5 [t_{2g}], Q_2 [e_g]) are not quantitatively obtained by this method, but qualitatively it is clear that their effect is substantial. For example, the ν_5 ($J_5 = 3/2$) linear JT level is split by 50 cm^{-1} by these quadratic terms whereas the splitting of the ν_5 ($J_5 = 3/2$) - ν_5 ($J_5 = 1/2$) levels induced by linear JT terms is only ~100 cm^{-1} (see Table 4). Thus, the conclusion reached previously[1,2] that the linear JT theory does not adequately describe the JT interactions observed in metal hexafluorides is strongly supported by these data.

A comparison of the JT behavior of the Γ_{8g} ($^2T_{1g}$) (1.6 μ) state of IrF_6 with that of the Γ_{8g} of ReF_6[1] and the Γ_{8g} ($^2T_{2g}$) (0.6 μ) state of IrF_6[2] is of interest. The parameters which can be compared are: D_5, Q_5 [a_{1g}], (Q_5 [e_g], Q_5 [t_{2g}]), D_2, Q_2 [a_{1g}], Q_2 [e_g]. (Q_5 [e_g], Q_5 [t_{2g}]) represents the combined effect of the two terms.

A comparison of the parameters is as follows:

IrF_6 (Γ_{8g} ($^2T_{1g}$) - 1.6 μ) vs. IrF_6 (Γ_{8g} ($^2T_{2g}$) - 0.6 μ)

$$D_5^{1.6\mu} > D_5^{0.6\mu}$$

$$Q_5^{1.6\mu}[a_{1g}] < Q_5^{0.6\mu}[a_{1g}]$$

$$(Q_5^{1.6\mu}[e_g], Q_5^{1.6\mu}[t_{2g}]) > (Q_5^{0.6\mu}[e_g], Q_5^{0.6\mu}[t_{2g}])$$

and

IrF_6 (Γ_8 ($^2T_{1g}$)) vs. ReF_6 (Γ_{8g})

$D_5^{1.6\mu} \sim D_5^{ReF_6}$

$Q_5^{1.6\mu}[a_{1g}] \sim Q_5^{ReF_6}[a_{1g}]$

$(Q_5^{1.6\mu}[e_g], Q_5^{1.6\mu}[t_{2g}]) > (Q_5^{ReF_6}[e_g], Q^{ReF_6}[t_{2g}])$

$D_2^{1.6\mu} > D_2^{ReF_6}$

$Q_2^{1.6\mu}[a_{1g}] < Q_2^{ReF_6}[a_{1g}]$

$Q_2^{1.6\mu}[e_g] \sim Q_2^{ReF_6}[e_g]$.

One can conclude from this summary of vibronic parameters that the combined $(Q_5^{1.6\mu}[e_g], Q_5^{1.6\mu}[t_{2g}])$ terms are the largest ones of this type. Moreover, they are larger than $Q_5^{1.6\mu}[a_{1g}]$, which is the opposite of the behavior seen in the other states.

A comparison of other JT-related characteristics of the two IrF_6 states is also helpful. The ν_5 components of the Γ_{8g} ($^2T_{2g}$) state are found to preserve the low-symmetry electronic crystal field splitting observed at the origin[2], while in the present case, the crystal field splittings of ν_5 components are quenched to some extent. For example, the ν_5 (J = 1/2) state is split by 26.7 cm^{-1} instead of the 34.6 cm^{-1} that the origin is split. Such behavior is consistent with the magnitudes of the D_5 parameters ($D_5^{1.6\mu}$ = 0.13, $D_5^{0.6\mu}$ = 0.03) and the assumption that IrF_6 experiences a crystal field of approximately D_{4h} symmetry.[2] As pointed out in Reference 1, in this case the ν_5 components approximately carry the origin splitting, but the approximation improves as D_5 decreases. The JT activity of ν_2 in the Γ_{8g} ($^2T_{1g}$) state

might also contribute to the different crystal field behavior; under these conditions an admixture of ν_2 character into the ν_5 levels would cause partial crystal field quenching.[1] Large quadratic terms such as ($Q_5^{1.6\mu}[e_g]$, $Q_5^{1.6\mu}[t_{2g}]$) might also contribute to this quenching. Another observation consistent with $D_5^{1.6\mu} > D_5^{0.6\mu}$ is that the intensity in the $2\nu_5$ region is significantly greater for the 1.6μ transition (Γ_{8g} ($^2T_{1g}$)).

Finally, the different crystal field behavior for ν_5 observed in different Γ_8 states of IrF_6 and ReF_6 supports the contention that it is the molecular JT effect that dominates the distortion and not the low symmetry crystal field. It is therefore suggested that these data and conclusions should in general apply to the free O_h symmetry molecule.

IV. CONCLUSION

Absorption and electronic Raman spectroscopy have been used to elucidate the Jahn-Teller interaction in the Γ_{8g} ($^2T_{1g}$) state at 1.6μ of IrF_6. As was found previously[1,2] for the Γ_8 ($^2T_{2g}$) state of IrF_6 and the ground Γ_8 state of ReF_6, linear JT theory inadequately describes the experimental observations. In this case, however, different quadratic terms are found to be dominant, i.e., $(Q_5^{1.6\mu}\ [e_g],\ Q_5^{1.6\mu}\ [t_{2g}]) > Q_5^{1.6\mu}\ [a_{1g}]$. Both quadratic and crystal effects relax the strict linear JT optical selection rules such that all possible transitions to JT active vibronic components are observed.

REFERENCES

1. G. R. Meredith, J. D. Webb, E. R. Bernstein, Mol. Phys., 34, 995 (1977).

2. E. R. Bernstein, J. D. Webb, Mol. Phys., in press.

3. E. R. Bernstein, G. R. Meredith, J. D. Webb, J. Chem Phys., in press.

4. J.C.D. Brand, G. L. Goodman, B. Weinstock, J. Mol. Spec. 37, 464 (1971).

5. E. R. Bernstein, G. R. Meredith, J. Chem. Phys. 64, 375 (1976).

6. J. A. Koningstein, Introduction to the Theory of the Raman Effect (Reidel, Holland, 1972).

7. M. S. Child, H. C. Longuet-Higgins, Phil. Trans. Roy. Soc. 254A, 259 (1961).

8. E. R. Bernstein, G. R. Meredith, Chem. Phys. 24, 289-299, 301-309, 311-325 (1977).

Table 1. Electronic Raman spectrum of the Γ_{8g} ($^2T_{1g}$) state of IrF_6 in a MoF_6 host crystal at a bath temperature of 1.6 K. The slit widths correspond to about 10 cm^{-1}; the intense lines can be measured with an uncertainty of $\pm$ 1 cm^{-1} whereas the weaker lines are only accurate to $\pm$ 3 cm^{-1}.

σ (cm^{-1})(a) Vacuum	$\Delta\sigma$ (cm^{-1})	I (b)	FWHH (c) (cm^{-1})	Assignment (d)
6110	0	4000	10	Origin (a)
6138	28	3200	12	Origin (b)
6298	188	30	10	
6343	233	25	--	ν_5 (J_5 = 3/2); ν_4 (a,h)
6363	253	60	30	
6423	313	45		ν_5 (J_5 = 1/2)
6431	321	55		ν_5 (a, h)
6445	335	50		ν_5 (J_5 = 1/2)
6692	582	50		ν_2 (J_2 = 3/2)
6705	595	60		
6796	686	280		ν_2 (J_2 = 1/2)
6805	695	320		
6831	721	30		ν_3 (a, h)

(a) Stokes shift from exciting laser line (either 5400 or 5500 Å).

(b) Approximate number of photon counts per second under the experimental conditions (see Section II).

(c) FWWW = full width at half height.

(d) The notation ν_i (a, h) implies that ν_i of the host (MoF_6) is built on origin (a).

Table 2. Absorption spectrum of the Γ_{8g} ($^2T_{1g}$) state of IrF_6/MoF_6 at 1.6 K. Frequencies are given in vacuum wavenumbers and are accurate to $\pm$ 0.1 cm^{-1} for sharp lines.

σ (cm^{-1}) Vacuum	$\Delta\sigma(cm^{-1})$	$I^{(a)}$	FWHH$^{(b)}$(cm^{-1})	Assignment$^{(c)}$
6109.6 (16363.3 Å)	0.0	M	$\leq$ 0.6	Origin (a)
6144.2	34.6	S	2.5	Origin (b)
6305.0	195.4	M	1.6	ν_5^1 (J_5 = 3/2)
6312.2	202.6	S	2.4	ν_6 (a)
6322.8	213.3	W	1.6	ν_5^2 (J_5 = 3/2)
6344.6	235.1	S	1.6	ν_5^3 (J_5 = 3/2)
6346.9	237.4	S	1.6	ν_6(b)
6355.3	245.7	S	5.6	ν_5^4 (J_5 = 3/2)
6365.4	255.8	W		
6373.1	236.6	W		ν_4(a, h)
6377.0	267.4	W		
6389.8	280.3	W		$2\nu_6$(a, h)
6394.4	284.9	M	2.8	ν_4(b, h)
6400.7	291.1	S	4.0	ν_4(a)
6422.0	312.5	M	2.4	ν_5^5(a) (J_5 = 1/2)$^{(d)}$
6428.0	318.4	M	10.0	ν_4(b), ν_5(a,h)
6430.3	320.8	M		
6448.8	339.2	M	2.8	ν_5^6 (J_5 = 1/2)$^{(d)}$
6510.4	400.9	W		
6516.9	407.3	W		$2\nu_6$
6527.6	418.0	W		

Table 2. (continued)

σ (cm^{-1}) Vacuum	$\Delta\sigma$(cm^{-1})	I [a]	FWHH[b] (cm^{-1})	Assignment[c]
6534.6	425.1	W		
6544.2	434.6	W	2.7	$2\nu_5$ (J_5 = 5/2)
6551.3	441.8	W	2.7	
6558.0	448.5	W	12.0	
6562.3	452.7	W		
6575.0	465.5	W		
6581.7	472.2	W	8.0	
6595.6	486.0	W		(ν_6 + ν_4) (a)
6621.2	511.7	W		
6626.5	517.0	W		(ν_6 + ν_4) (b)
6637.1	527.5	M	15.0	$2\nu_5$ (J_5 = 1/2)[d]
6664.8	555.2	W	10.0	
6673.3	563.7	W		
6689.6	580.0	W		ν_2 (J_2 = 3/2)
6700.0	590.5	W		$2\nu_5$ (J_5 = 3/2)
6706.5	596.9	W	17.0	ν_2 (J_2 = 3/2)
6716.7	607.1	W		$2\nu_5$ (J_5 = 3/2)
6726.3	616.7	W	13.0	$2\nu_5$ (J_5 = 3/2)
6755.8	646.2	W		
6766.7	657.1	W		
6788.9	679.4	W		
6795.4	685.8	W	4.3	ν_2 (J_2 = 1/2)
6801.6	692.0	M	1.6	
6809.9	700.4	M	4.8	ν_1(a) — ν_3(a,h)
6819.4	709.8	W		

Table 2. (continued)

σ (cm^{-1}) Vacuum	$\Delta\sigma$(cm^{-1})	I[a]	FWHH[b] (cm^{-1})	Assignment[c]
6842.9	733.4	W	9.0	ν_1(b); ν_3(b,h)
6876.4	766.8	W		
6888.8	779.2	W		
6894.2	784.7	W		
6988.4	878.8	W		
7003.0	893.5	W	15.0	($\nu_1 + \nu_5^1$) (a)
7016.0	906.4	W	14.0	($\nu_1 + \nu_6$) (a)
7025.9	916.2	W		($\nu_1 + \nu_5^2$) (a)

(a) Relative intensities: S = strong, M = medium, W = weak.

(b) FWHH = full width at half-height.

(c) The notation ν_i (a) means the ν_i mode built on the (a) origin. ν_i (b) implies ν_i built on origin (b). ν_i (a,h) means that mode ν_i of the host (MoF_6) is built on origin (a). These latter two-particle transitions are discussed in more detail in references 1, 2, and 5.

(d) In GVC theory (see text) these levels can be identified as components of Γ_{8g} vibronic states.

Table 3. A Comparison of Absorption and Electronic Raman Data.

Electronic Raman	Absorption	Assignments
188	195.4	ν_5 (J_5 = 3/2)
	213.3	
233	235.1	
253	245.7[(a)]	
313	312.5	ν_5 (J_5 = 1/2)
335	339.2	
582	580.0	ν_2 (J_2 = 3/2)
595	596.9	
686	685.8	ν_2 (J_2 = 1/2)
695	692.0	

(a) Region congested by presence of host-related features. (See text for discussion and Tables 1 and 2.)

Table 4. Comparison of a ν_2-ν_5 linear Jahn-Teller (LJT) calculation[1] with centers-of-gravity of various groups of experimentally observed transitions (see Table 2). The parameter values in the calculation are the following: $D_5 = 0.13$, ν_5^0 (Q_5 [a_{1g}]) = 255 cm^{-1}, $D_2 = 0.03$, ν_2^0 (Q_2 [a_{1g}]) = 630 cm^{-1}.

LJT Level	$E_{Calc}(cm^{-1})$	$E_{LJT}^{(a)}$ (cm^{-1})	$E_{\nu}^{(c)}(cm^{-1})$
ν_5 (J_5 = 3/2)	218	220(50)	252
ν_5 (J_5 = 1/2)	319	312[b]	
$2\nu_5$ (J_5 = 5/2)	442	452(38)	515
$2\nu_5$ (J_5 = 1/2)	509	527[b]	
$2\nu_5$ (J_5 = 3/2)	584	604(27)	
ν_2 (J_2 = 3/2)	603	587(17)	638
ν_2 (J_2 = 1/2)	696	689[b]	

(a) Centers-of-gravity of various groups of ν_5 and ν_2 components; these approximate the LJT levels which would be observed in the absence of quadratic JT splitting. The parenthetical numbers are the maximum quadratic splitting.

(b) The lower component of the split Γ_8 vibronic state is used here since the splitting can be identified as a crystal field splitting rather than as quadratic JT. The weight factor of the state is then doubled in the averaging process.

(c) Centers-of-gravity of the LJT levels.

Figure 1.

Origin region of Γ_{8g} ($^2T_{1g}$) state of IrF_6/MoF_6 as observed in electronic Raman scattering. The two peaks are components of the Γ_{8g} state which is split by a low symmetry crystal field.

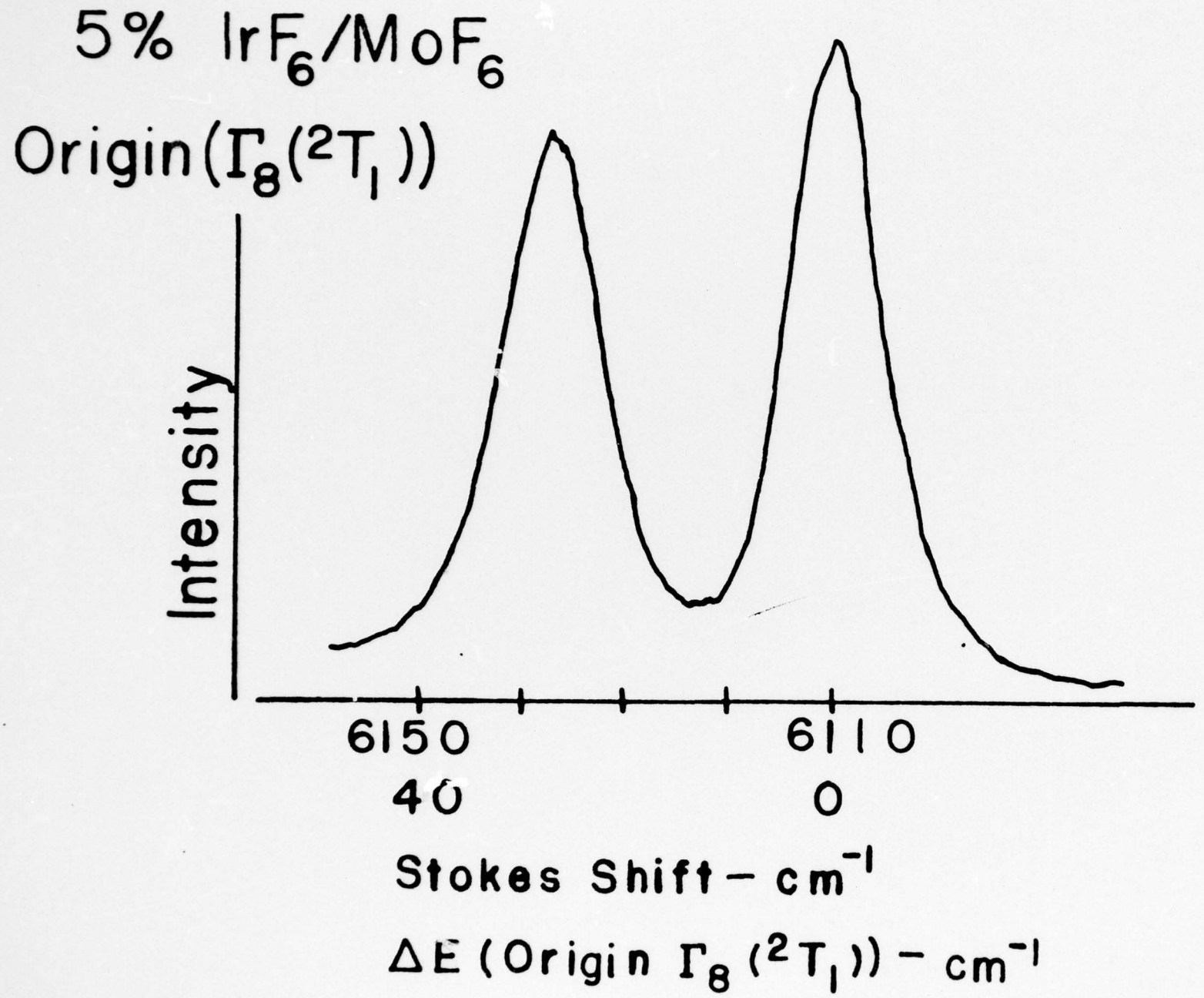
5% IrF_6/MoF_6
Origin($\Gamma_8(^2T_1)$)
Intensity
6150
40
6110
0
Stokes Shift – cm^{-1}
ΔE (Origin $\Gamma_8(^2T_1)$) – cm^{-1}

Figure 2.

The electronic Raman spectrum of the vibrational bending region of the Γ_{8g} ($^2T_{1g}$) electronic state of IrF_6/MoF_6. These peaks are identified as Jahn-Teller-split ν_5 (t_{2g}) components. Tables 1 and 3 contain detailed assignments.

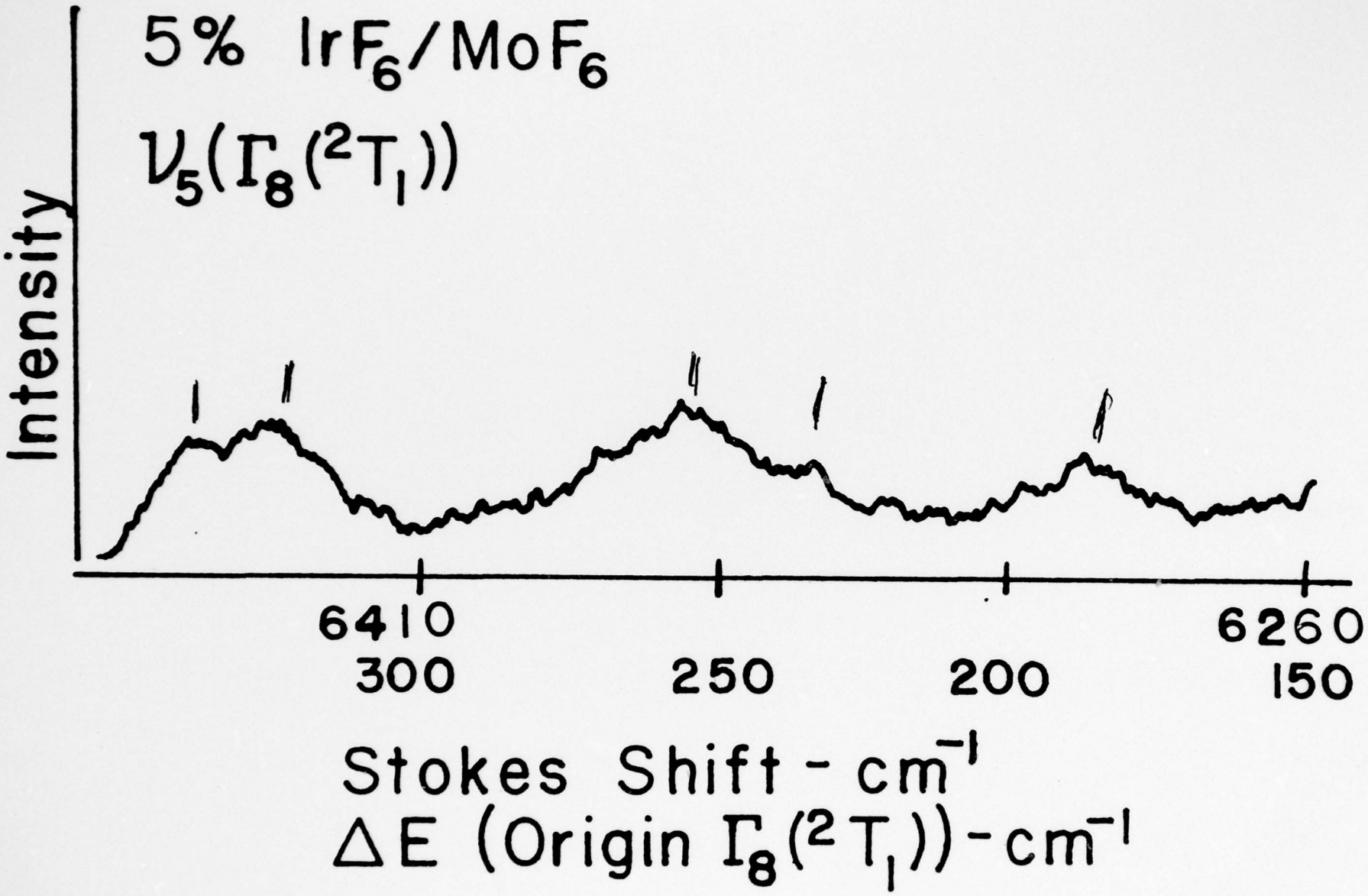
5% IrF6/MoF6
ν5(Γ8(2T1))
Intensity
6410
6260
300
250
200
150
Stokes Shift - cm-1
ΔE (Origin Γ8(2T1)) - cm-1

Figure 3.

The electronic Raman spectrum of the vibrational stretching region of the Γ_{8g} ($^2T_{1g}$) electronic state of IrF_6/MoF_6. The main features are identified as ν_2 (e_g) components. A slower scan, with higher time constant, of the feature at 690 cm^{-1} shows that it consists of two components (see Table 1).

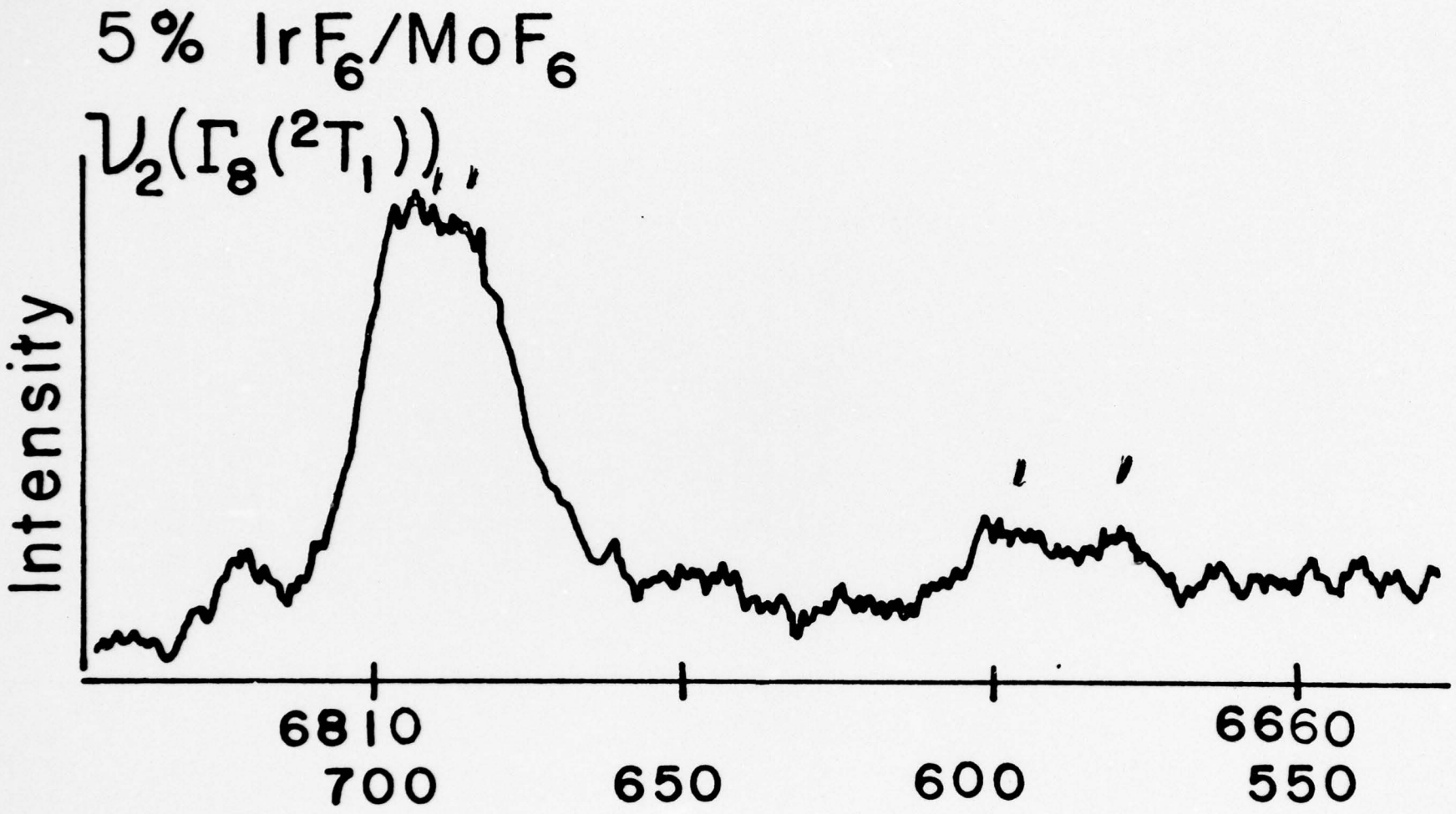
5% IrF6/MoF6
ν2(Γ8(2T1))
Intensity
6810
6660
700
650
600
550
Stokes Shift - cm-1
ΔE (Origin Γ8(2T1)) - cm-1

Figure 4.

Absorption spectrum of the vibrational bending region of the Γ_{8g} ($^2T_{1g}$) electronic state of IrF_6/MoF_6. Compare with the corresponding electronic Raman spectrum in Figure 2; the ν_6 and ν_4 features are absent there. Note that the ν_5 ($n_5 = 1$) vibration is split by both a linear and quadratic Jahn-Teller effect. The linear term produces $J_5 = 3/2$ and $J_5 = 1/2$ levels, while the quadratic and low symmetry crystal field terms give the further splittings of these linear JT components.

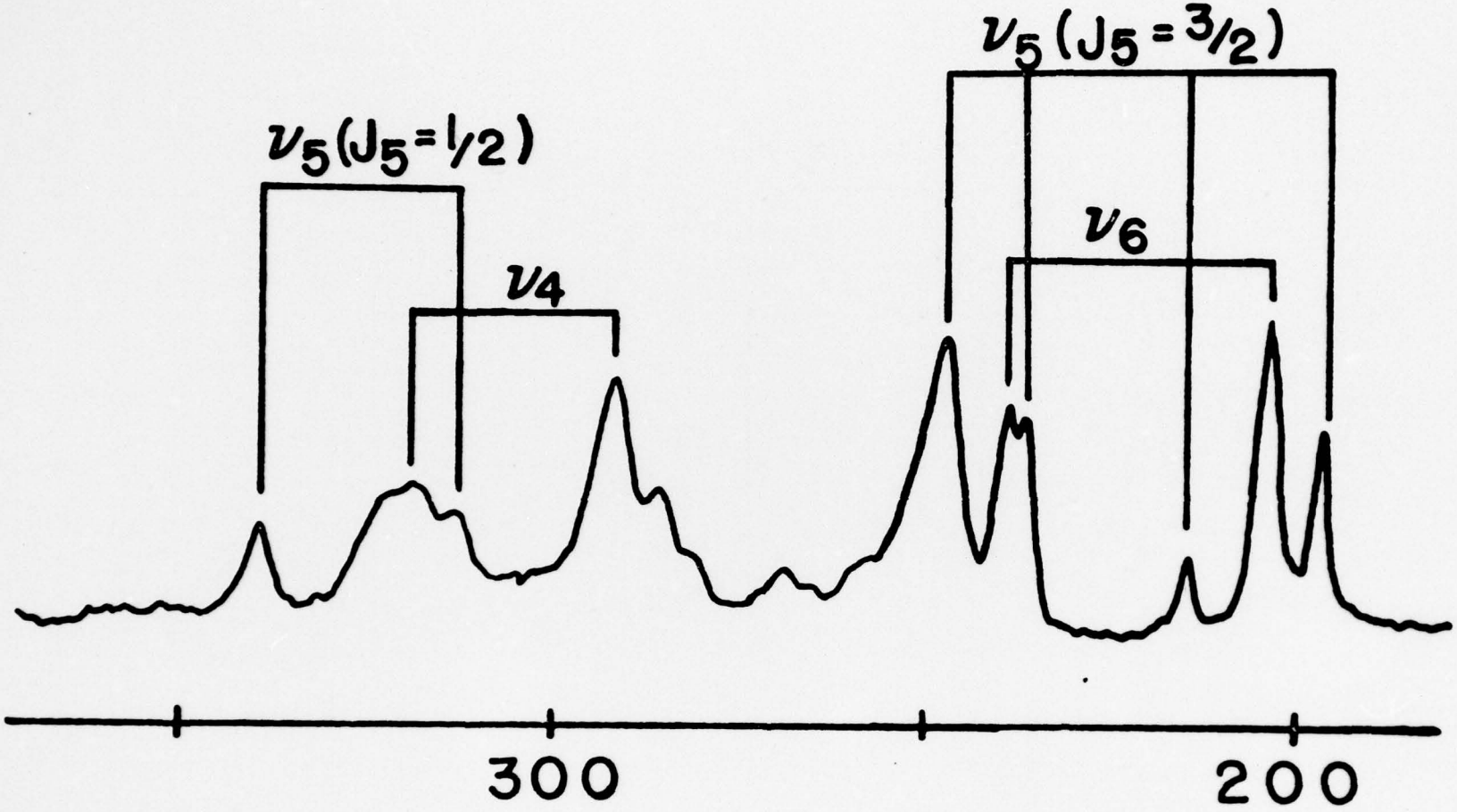

ΔE (origin $\Gamma_{8g}(^2T_{1g})$)/cm^{-1}

Figure 5.

Absorption spectrum of the vibrational combination and overtone bending region in the Γ_{8g} ($^2T_{1g}$) electronic state of IrF_6/MoF_6. Most of the features are identified as components of the Jahn-Teller active vibrations, ν_2 (e_g) or ν_5 (t_{2g}). Note the groupings of the peaks; these serve to identify the positions of the linear Jahn-Teller (LJT) levels in the absence of quadratic JT splitting. (See text and Table 4.)

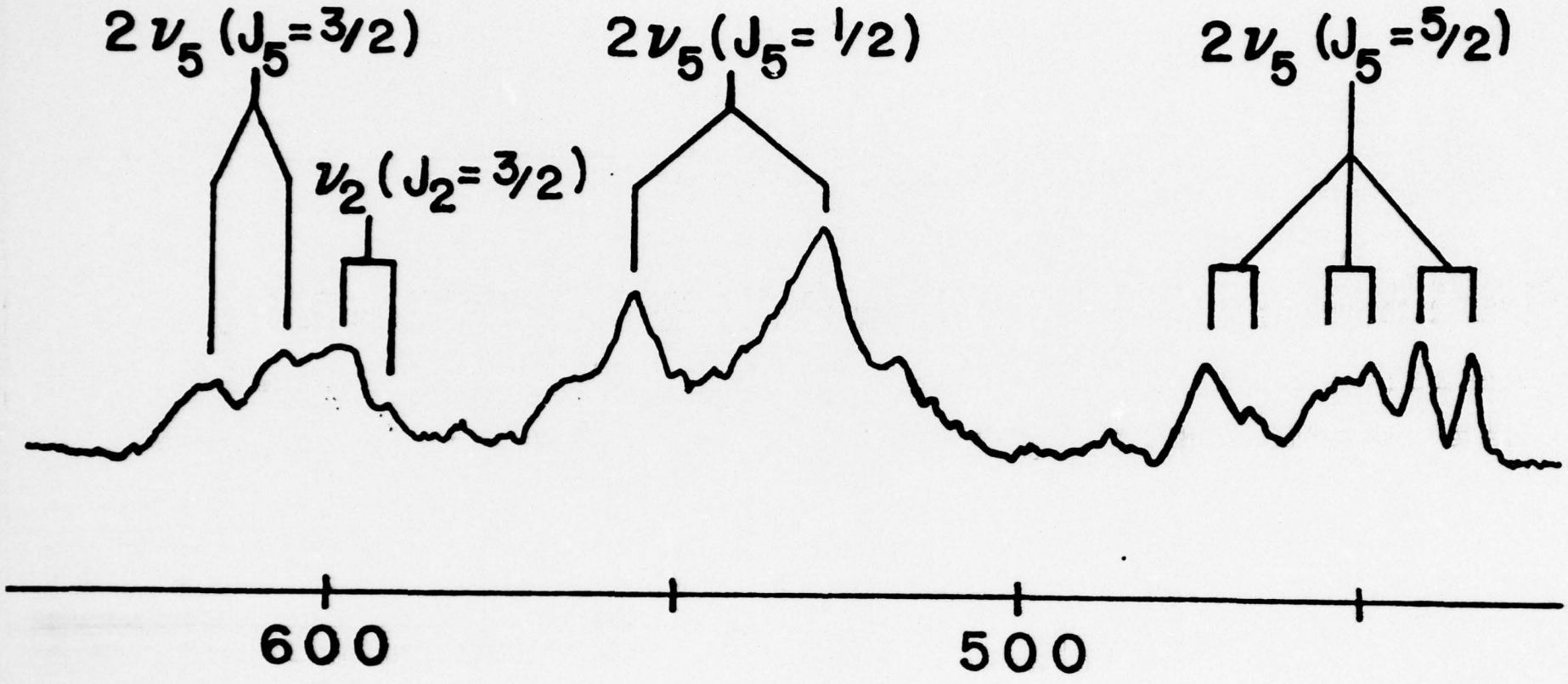
$2\nu_5 (J_5=3/2)$
$\nu_2 (J_2=3/2)$
$2\nu_5 (J_5=1/2)$
$2\nu_5 (J_5=5/2)$
600
500
ΔE (origin $\Gamma_{8g}(^2T_{1g})$)/cm^{-1}

Figure 6.

Absorption spectrum of IrF_6/MoF_6 in the vibrational stretching region of the Γ_{8g} ($^2T_{1g}$) electronic state of IrF_6/MoF_6. The splitting of the $J_2 = 1/2$ component of ν_2 (e_g) is caused by the low symmetry crystal field. Its value (about 6 cm^{-1}) has been substantially reduced from the origin splitting by vibronic interaction.

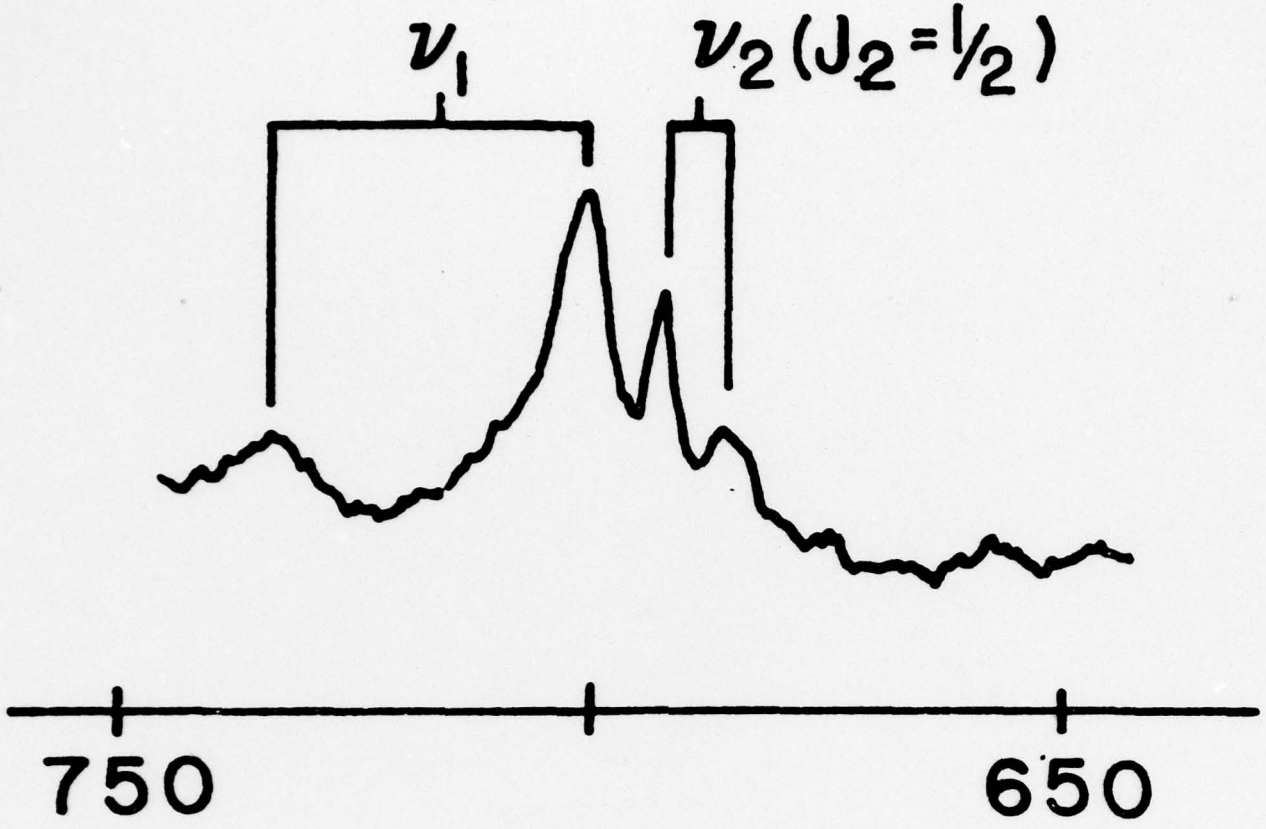

ΔE (origin $\Gamma_{8g}(^2T_{1g})$)/cm^{-1}

TECHNICAL REPORT DISTRIBUTION LIST

	No. Copies
Office of Naval Research Arlington, Virginia 22217 Attn: Code 472	2
Office of Naval Research Arlington, Virginia 22217 Attn: Code 1021P 1	6
ONR Branch Office 536 S. Clark Street Chicago, Illinois 60605 Attn: Dr. Jerry Smith	1
ONR Branch Office 715 Broadway New York, New York 10003 Attn: Scientific Dept.	1
ONR Branch Office 1030 East Green Street Pasadena, California 91106 Attn: Dr. R. J. Marcus	1
ONR Branch Office 760 Market Street, Rm. 447 San Francisco, California 94102 Attn: Dr. P. A. Miller	1
ONR Branch Office 495 Summer Street Boston, Massachusetts 02210 Attn: Dr. L. H. Peebles	1
Director, Naval Research Laboratory Washington, D.C. 20390 Attn: Code 6100	1
The Asst. Secretary of the Navy (R&D) Department of the Navy Room 4E736, Pentagon Washington, D.C. 20350	1
Commander, Naval Air Systems Command Department of the Navy Washington, D.C. 20360 Attn: Code 310C (H. Rosenwasser)	1
Defense Documentation Center Building 5, Cameron Station Alexandria, Virginia 22314	12
U.S. Army Research Office P.O. Box 12211 Research Triangle Park, N.C. 27709 Attn: CRD-AA-IP	1
Naval Ocean Systems Center San Diego, California 92152 Attn: Mr. Joe McCartney	1
Naval Weapons Center China Lake, California 93555 Attn: Head, Chemistry Division	1
Naval Civil Engineering Laboratory Port Hueneme, California 93041 Attn: Mr. W. S. Haynes	1
Professor O. Heinz Department of Physics & Chemistry Naval Postgraduate School Monterey, California 93940	1
Dr. A. L. Slafkosky Scientific Advisor Commandant of the Marine Corps (Code RD-1) Washington, D.C. 20380	1
Office of Naval Research Arlington, Virginia 22217 Attn: Dr. Richard S. Miller	1

TECHNICAL REPORT DISTRIBUTION LIST

	No. Copies		No. Copies
Dr. M. A. El-Sayed University of California Department of Chemistry Los Angeles, California 90024	1	Dr. G. B. Schuster University of Illinois Chemistry Department Urbana, Illinois 61801	1
Dr. M. W. Windsor Washington State University Department of Chemistry Pullman, Washington 99163	1	Dr. E. M. Eyring University of Utah Department of Chemistry Salt Lake City, Utah	1
Dr. E. R. Bernstein Colorado State University Department of Chemistry Fort Collins, Colorado 80521	1	Dr. A. Adamson University of Southern California Department of Chemistry Los Angeles, California 90007	1
Dr. C. A. Heller Naval Weapons Center Code 6059 China Lake, California 93555	1	Dr. M. S. Wrighton Massachusetts Institute of Technology Department of Chemistry Cambridge, Massachusetts 02139	1
Dr. M. H. Chisholm Princeton University Department of Chemistry Princeton, New Jersey 08540	1	Dr. M. Rauhut American Cyanamid Company Chemical Research Division Bound Brook, New Jersey 08805	1
Dr. J. R. MacDonald Naval Research Laboratory Chemistry Division Code 6110 Washington, D.C. 20375	1		